Title: Current and future biomass carbon uptake in Boston's urban forest

Authors: Andrew Trlica[a,*], Lucy R. Hutyra[b], Luca L. Morreale[c], Ian A. Smith[d], and Andrew B. Reinmann[e,f,g]

[a]Boston University, Department of Earth & Environment, 685 Commonwealth Ave., Boston, Massachusetts, USA. atrlica@bu.edu

[b]Boston University, Department of Earth & Environment, 685 Commonwealth Ave., Boston, Massachusetts, USA. lrhutyra@bu.edu

[c]Boston University, Department of Earth & Environment, 685 Commonwealth Ave., Boston, Massachusetts, USA. lmorreal@bu.edu

[d]Boston University, Department of Earth & Environment, 685 Commonwealth Ave., Boston, Massachusetts, USA. iasmith@bu.edu

[e]Environmental Sciences Initiative, CUNY Advanced Science Research Center, 85 Saint Nicholas Terr., New York, New York, USA. areinmann@gc.cuny.edu

[f]PhD Program in Earth and Environmental Science, The Graduate Center, CUNY, 365 First Ave., Room 4306, New York, New York, USA. areinmann@gc.cuny.edu

[g]Department of Geography and Environmental Science, Hunter College, 695 Park Ave., Room 1006 HN, New York, New York, USA. areinmann@gc.cuny.edu

*Corresponding author. Email address: atrlica@bu.edu (A. Trlica)

Highlights:

- Estimated tree C uptake was 56% lower without accounting for canopy configuration.
- Median C uptake was 0.5 (0–3.1) MgC ha^{-1} yr^{-1}, Boston total was 10.9 (6.7–16.2) GgC yr^{-1}.
- The majority (85%) of canopy area was within 10 m of an edge.
- High-Density Residential areas hosted 49% of urban forest biomass C uptake.
- Planting additional trees resulted in greater C uptake vs. preserving larger trees.

Graphical Abstract:

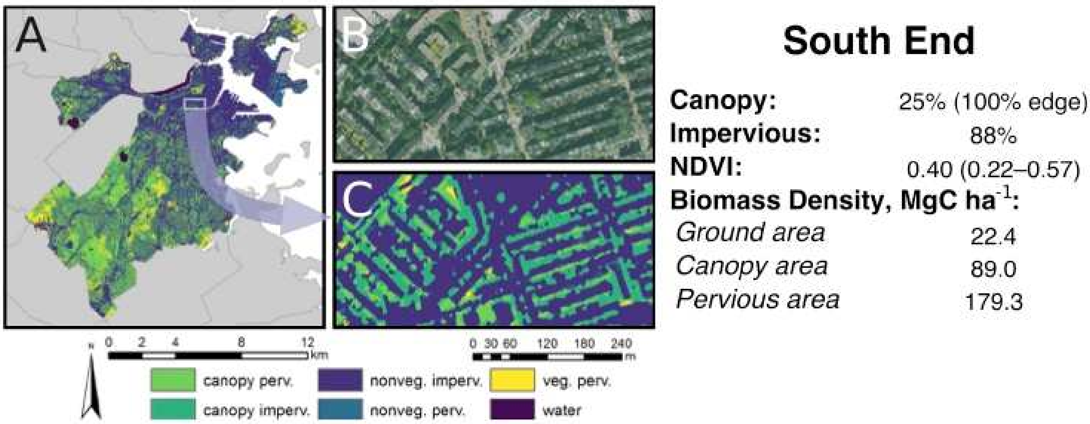

Abstract

Ecosystem services provided by urban forests are increasingly included in municipal-level responses to climate change. However, the ecosystem functions that generate these services, such as biomass carbon (C) uptake, can differ substantially from nearby rural forest. In particular, the scaled effect of canopy spatial configuration on tree growth in cities is uncertain, as is the scope for medium-term policy intervention. This study integrates high spatial resolution data on tree canopy and biomass in the city of Boston, Massachusetts, with local measurements of tree growth rates to estimate the magnitude and distribution of annual biomass C uptake. We further project C uptake, biomass, and canopy cover change to 2040 under alternative policy scenarios affecting the planting and preservation of urban trees. Our analysis shows that 85% of tree canopy area was within 10 m of an edge, indicating essentially open growing conditions. Using growth models accounting for canopy edge effects and growth context, Boston's current biomass C uptake may be approximately double (median 10.9 GgC yr^{-1}, 0.5 MgC ha^{-1} yr^{-1}) the estimates based on rural forest growth, much of it occurring in high-density residential areas. Total annual C uptake to long-term biomass storage was equivalent to <1% of estimated annual fossil CO_2 emissions for the city. In built-up areas, reducing mortality in larger trees resulted in the highest predicted increase in canopy cover (+25%) and biomass C stocks (236 GgC) by 2040, while planting trees in available road margins resulted in the greatest predicted annual C uptake (7.1 GgC yr^{-1}). This study highlights the importance of accounting for the altered ecosystem structure and function in urban areas in evaluating ecosystem services. Effective municipal climate responses should consider the substantial fraction of total services performed by trees in developed areas, which may produce strong but localized atmospheric C sinks.

Keywords: urban forest, canopy fragmentation, carbon uptake, climate adaptation, street trees, ecosystem services

Abbreviations: BAU – Business-as-usual; DBH – diameter at breast height; LULC – land use/land cover; PL – Preserve Largest; STP – Street Tree Planting

1 Introduction

As urban populations expand worldwide, pressure is rising on local ecosystem services to both provide a livable environment in cities and to address the drivers and effects of global climate change (Seto et al., 2012). Urban vegetation performs a suite of these ecosystem services, including key regulatory functions like carbon (C) uptake and storage, moderation of temperature extremes (McDonald et al., 2019), and potentially air pollution mitigation through ozone and particulate matter capture (Roy et al., 2012). Municipal authorities are increasingly assuming a role in mounting a social response to climate change (Castán Broto, 2017), and policy-makers and researchers show growing interest in better quantifying and managing the multiple ecosystem services provided by green spaces and urban vegetation (Kremer et al., 2016; Lovell and Taylor, 2013; Niemelä, 2014). Toward this end, researchers have recently called for more intensive study of these novel and heterogeneous socio-ecological systems and their spatiotemporal organization, both in their own right and in the interest of maintaining the well-being of growing and at-risk urban populations (Alberti, 2015; Groffman et al., 2017; Hutyra et al., 2014; Zhou et al., 2019).

Services related to urban vegetation and their role in climate change adaptation and emissions mitigation have attracted particular policy interest (Gómez-Baggethun and Barton, 2013; Larondelle and Haase, 2013; Lovell and Taylor, 2013). In line with several other cities and municipal alliances like the C40 coalition developing climate responses (Broto and Bulkeley, 2013), Boston, for example, has included the expansion of green spaces and tree canopy cover as strategies in its climate adaptation and emissions reductions plans (Walsh, 2014). However, despite prominent campaigns in several US cities to plant additional urban trees, canopy cover has declined in many urban areas (Nowak and Greenfield, 2012). And in the wake of broad-scale tree planting and other "urban greening" proposals, researchers have highlighted persistent uncertainties in estimating the amount and value of services, the quality and specificity of data and modeling used to estimate services, potential tradeoffs with other disservices such as increased water consumption and allergen production, and the capacity of vegetation C uptake to meaningfully offset comparatively large local fossil C emissions (Pataki, 2013; Pataki et al., 2011; Pincetl et al., 2013). There is moreover little support, beyond fairly generalized models such as UFORE/i-Tree Eco (Nowak et al., 2008), to help urban decision makers assess current forest services, predict the impacts of urban greening policies on net greenhouse gas emissions, or optimize the production of multiple services against their tradeoffs and costs (Escobedo et al., 2011).

Ecosystem services are a product of ecosystem functions, like evapotranspiration or C uptake, that serve human wellbeing, and as such take place in a specific spatiotemporal setting (Escobedo et al., 2011). Many of the services performed by urban ecosystems relevant in climate change mitigation and resiliency planning are related to the amount of live tree biomass present, its rate of growth, and canopy cover and volume (Nowak et al., 2008; Ziter et al., 2019). These services are generated within heterogeneous forest or "savannah-like" ecosystems, the structure and function of which are determined by biophysical setting, human socioeconomic spatial patterns, and inherited legacies of historic and ongoing human activity (Dobbs et al., 2017; Ossola and Hopton, 2018; Roman et al., 2018). Given its complexity and recency as a study domain, our understanding of urban forest function and its spatial distribution contains considerable uncertainty, reflected in results from urban studies that contradict expectations derived from rural analogues. Despite some ambiguity in definition, "urban" ecosystems can contain substantial biomass concentrations, varying widely with land cover and use (Davies et al., 2011; Raciti et al., 2012; Rao et al., 2013). Tree canopy morphology may differ notably in the same species grown in different cities and between urban- and rural-grown individuals (McPherson and Peper, 2012). Growth rates in street- and park trees can exceed or fall short of comparable trees in nearby rural settings (Briber et al., 2015; Gregg et al., 2003; Pretzsch et al., 2017; Searle et al., 2012), while mortality rates tend to be higher in smaller diameter- and street trees (Roman et al., 2014; Smith et al., 2019). Tree growth in remnant urban forest fragments can be significantly enhanced near canopy edges (Reinmann and Hutyra, 2017). Growing seasons under the influence of the urban heat island effect may be longer than nearby rural areas (Melaas et al., 2016).

Existing studies of urban forest growth and C uptake contain uncertainties in accounting for local urban-specific growth rates and the spatial arrangement or extent of tree cover. Several studies estimating services from urban trees have used the Urban Forest Effects (UFORE) model (Nowak et al., 2008), scaling plot-level tree measurements to the broader urban landscape using spatial proxies like mapped land use/cover classes and applying generic corrections for urban-related growth effects (Escobedo and Nowak, 2009; Nowak et al., 2013; Strohbach et al., 2012). A study of tree C storage and sequestration in Los Angeles and Sacramento scaled plot-level biomass inventories to canopy coverage as determined from 2.4 m resolution satellite observations, but lacked error estimation and relied upon generalized growth projections to determine annual C uptake (McPherson et al., 2013). Other studies have only partially estimated C storage and uptake via inventory of sub-populations of urban trees such as street trees or greenspaces (Brack, 2002; Russo et al., 2014; van Doorn and McPherson, 2018). As part of their CO_2 emissions inventory for Salt Lake City Pataki et al. (2009) used a simple age cohort-based growth model for tree biomass C uptake derived from local tree inventory data, with forest extent determined from 30 m spatial resolution Landsat imagery. Other research has estimated temporal change in urban C storage with historical land conversion (Hutyra et al., 2011), and projected future functional shifts under varying mortality and recruitment scenarios for specific tree sub-populations (Smith et al., 2019).

Working from a photosynthetic light-use efficiency framework, several other studies have attempted to model urban vegetation C uptake based in part on light absorption: Miller et al. (2018) estimated gross primary productivity (a C flux not accounting for plant respiration losses) across the city of Minneapolis, Minnesota, based on limited sapflow and eddy covariance measurements corresponding to broad vegetation functional groups (e.g. deciduous trees, turf). They then scaled results spatially based on high-resolution classification maps of vegetation and land cover. Urban micrometeorological studies have partitioned C fluxes limited to the vicinity of measurement towers into vegetation components by adjusting for photosynthetic light absorption (Bellucco et al., 2017; Crawford et al., 2011). Urban vegetation C uptake has been estimated across urbanized areas via light-use models driven by coarse-scale remote-sensing data, but without reference to local observations of vegetation C uptake (Hardiman et al., 2017; Imhoff et al., 2004). Other research has estimated temporal change in urban C storage with historical land conversion (Hutyra et al., 2011), and projected future functional shifts under varying mortality and recruitment scenarios for specific tree sub-populations (Smith et al., 2019). However, a complete and adequately spatially resolved understanding of urban ecosystem function, incorporating empirical measures of urban forest extent, productivity, and structure, remains elusive., along with a In addition, this knowledge gap impedes a clear understanding of the potential to optimize urban ecosystem functions via policy.

Effective municipal climate preparedness and protection of urban environmental quality requires a more precise understanding of the local ecosystem functions like C storage and canopy coverage that drive critical services provision. Improved estimates of urban ecosystem function require knowledge of the spatial distribution and growth dynamics of the urban forest. This study combines local observations of tree growth and its relationship to canopy fragmentation with high-resolution maps of biomass and canopy distribution to estimate annual long-lived biomass C uptake in the urban landscape of Boston, Massachusetts. For contrast to estimates grounded in rural forest ecosystem function, we compare our urban-specific results to estimates based on tree growth measured in nearby rural forests. We finally simulate three policies differentially affecting the recruitment and mortality of urban trees to predict future potential trajectories of C uptake, biomass, and canopy cover change through 2040. Improving estimates of these indicators will deepen our understanding urban ecosystem functioning, and highlight the potential effects of green infrastructure policies on climate mitigation and preparedness, with the city of Boston as a specific test case.

2 Methods

2.1 Study area geodata

To develop our estimate of biomass C storage in Boston's urban trees, we employed a 1 m resolution gridded map of aboveground woody biomass and canopy presence for the municipal boundaries of Boston, Massachusetts, prepared using satellite multispectral and aerial LIDAR observations in the summer of 2006–2007 (Figure 1) (Raciti et al., 2014). We classified canopy pixels according to their pixel buffer distance from canopy patch edges using the Expand tool in ArcMap 10.4 (ESRI, 2014), with all pixels within 10 pixels (approximately 10 m) of a canopy edge classified as "edge" canopy. We combined biomass, canopy, and canopy edge maps with 1 m maps of land-use/land-cover (LULC) classification and impervious surface presence/absence prepared from aerial photographs (MassGIS, 2005). The LULC categories were Forest, Developed (non residential), High Density Residential, Low Density Residential, Other Vegetated, and Water, simplified from the LULC classification scheme used by MassGIS (2005) (Table S1). To represent tree-scale and larger ecosystem dynamics, we then aggregated the data to generate 30 m spatial resolution gridded maps of total biomass, fractional canopy and canopy edge area, fractional impervious area, and LULC classification by greatest combined class area per pixel. We also examined the sensitivity of estimates to differing spatial methods for evaluating pixel-level biomass density. We calculated biomass density at the 30 m pixel scale (MgC ha^{-1}) as (1) the biomass C present versus pixel area under tree canopy (canopy basis) (e.g. Nowak et al., 2013); (2) biomass C versus total pixel area (ground basis) (e.g. Ouimette et al., 2018); and (3) biomass C versus non-paved pixel area (pervious basis).

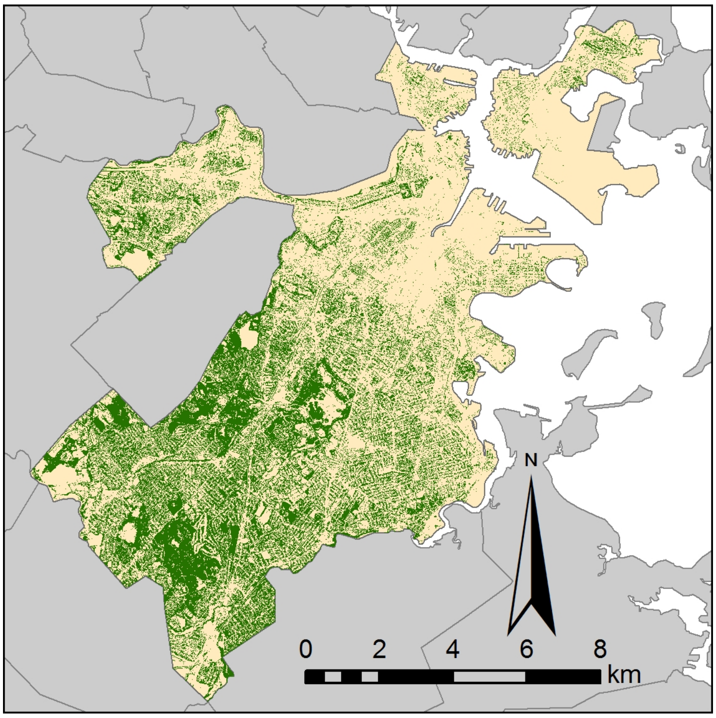

Figure 1: Boston study area showing tree canopy area (green).

2.2 Tree growth data

A linear mixed-model framework was used to estimate the relationship between stem diameter at breast height (DBH, cm) and growth rate (cm tree^{-1} yr^{-1}) for measurements of trees growing in rural forests (Rural Forest), urban forest fragments (Urban Forest), and open-grown street, park, and backyard trees (Street Tree) (Table S2). The Rural Forest growth model was based on repeated stem DBH measurements (n = 6,710 stems) from 2003–2015 in plots monitored under the USDA's Forest Inventory Analysis (FIA) program (USDA, 2019). The Urban Forest model was based on measurements in 2015 from eight forested test plots (n = 425 stems) located in nearby suburbs of Boston, subdivided based on their distance from long-lived canopy edges (<10m, 10–20 m, 20–30 m) (Reinmann and Hutyra, 2017). Rate of DBH change for Urban Forest was determined based on increment cores taken from a subset of stems in each plot (n = 195 cores). The Street Tree growth model was based on repeated measurements of stem DBH obtained for healthy live trees (n = 2,592 stems) growing along public rights-of-way in several zones across the city of Boston in 2006 and 2014 (Smith et al., 2019). Complete data collection protocols and discussion of model construction are available in the Supplemental.

2.3 Growth modeling

We used stem growth rates taken from the Rural Forest and Urban Forest models with the measured DBH of living stems present, via allometric equations, to determine the relationship between areal aboveground woody biomass density per test plot (MgC ha^{-1}) and its corresponding relative biomass gain rate (MgC yr^{-1} per MgC-biomass) (Tables S2 and S3; See Supplemental for allometric equations used and discussion of areal-basis growth model estimation). We then used the areal-basis growth models to predict annual rate of C gain in aboveground woody biomass for each 30 m map pixel by estimating relative biomass gain rate based on pixel biomass density, then multiplying the predicted biomass gain rate by pixel tree biomass C (MgC) to determine pixel annual biomass C gain (MgC $pixel^{-1}$ yr^{-1}), with 1,000 bootstrap resamples of coefficients in the areal-basis models to estimate error. For the Urban Forest model, growth factors and biomass gain were estimated for the canopy edge (<10m) and interior (10–30 m) biomass component of each pixel separately, using only the per-ha-canopy areal basis for biomass density.

Because of the sampling design of the Street Tree observations it was not possible to directly estimate an areal-basis model for biomass growth. As an alternative, for each pixel a collection of tree stems was simulated by randomly drawing (with replacement) a selection of stems from the Street Tree DBH measurements taken in the city of Boston (2,592 tree records). Valid stem collections approximated biomass to within the smaller of 100 kg or 10% of pixel total biomass (canopy area basis). Tree number per pixel was not fixed but tree collections were constrained to a total maximum basal area of 40 m^2 per ha of pixel canopy area (Reinmann and Hutyra, 2017). This simulation method was repeated to obtain 100 valid collections per pixel, recording DBH and taxon for each tree in each collection. (See Supplemental on simulation of pixel-level stem collections). The Street Tree stem growth model was then applied to a randomly chosen pixel stem collection, using urban-specific allometric equations to estimate biomass change (McPherson et al., 2016) (Table S4). This estimation approach was repeated for every pixel with 1,000 bootstrap resamples of the simulated stem collections and coefficients of the stem growth model, with the same growth model applied to all pixels in each resample. To complete the map-wide estimate of annual biomass C uptake, a composite "Hybrid Urban" estimate was generated by combining outputs of the Urban Forest model in pixels classed as "Forest" or containing >111 MgC ha^{-1} biomass with outputs of the Street Tree model for all other non-forest pixel types. This cutoff corresponded approximately to the biomass density of local rural forests (Fahey et al., 2005; Magill et al., 2004), and the threshold past which estimation based on the Street Tree simulation approach became computationally impractical. The Hybrid Urban results were contrasted to the annual biomass C uptake estimated using the Rural Forest model under both the canopy basis and ground basis for calculating biomass density.

2.4 Policy Projections

Three alternate scenarios for policies affecting urban ecosystem function were projected for 2006–2040 based on the simulated collections of street tree stems contained in Developed, HD Residential, and LD Residential pixels with <111 MgC ha^{-1} (77,955 pixels total). The three scenarios were: 1) Business as Usual (BAU) in which the 2006–2007 pixel simulations were projected to 2040 under assumptions of mortality risk and stem growth rate described above; 2) Preserve Largest (PL), in which mortality for all trees >40 cm DBH was reduced by 50% relative to their measured size-based annual mortality risk (Smith et al., 2019); and 3) Street Tree Planting (STP) in which approximately 170,000 small (5 cm DBH) street trees were added to the map total over the first 10 projection years, the maximum plausible ceiling of new trees that could be added based on the total non-canopied area available adjacent to Boston's surface streets. (See Supplemental for discussion of identifying plantable road buffer space).

For each pixel a randomly selected simulated stem collection was subjected to annual size-based mortality risk (Smith et al., 2019) and predicted growth rate based on the Street Tree growth model. In pixels in which a tree mortality occurred, or pixels under the STP scenario that simulated a new tree planting, new or replacement trees were simulated with 5 cm DBH and a taxon randomly selected from the Street Tree survey record. The trajectory of annual biomass growth, total biomass, stem number, and canopy area was projected for each policy for each scenario year. Each scenario timeline was run with 100 bootstrap resamples of the stem growth model coefficients applied uniformly across scenarios to provide an uncertainty distribution for each metric while remaining computationally tractable (See Supplemental for discussion of on procedures used for policy projection).

2.5 Analysis

We evaluated the significance of fixed effects in mixed models using a drop-one Chi-square test, with final models including the lowest-order polynomial with all terms significant ($p < 0.05$) (Zurr et al., 2011). Models were selected parsimoniously to include only significant terms and their lowest-order significant polynomials. Random effects for available covariates were fit for intercepts, as well as for slope terms whenever possible (Table S2). All data processing was performed in *ArcMap* 10.4 (ESRI, 2014) and in the *R* software package (R Core Team, 2017) including the packages *lme4* (Bates et al., 2015), *raster* (Hijmans, 2017), *data.table* (Dowle and Srinivasan, 2017), and *rgdal* (Bivand et al., 2017). Due to skewed distributions, median values were reported with upper and lower limits of the central 95% of values, and growth models were reported with Residual Standard Deviance (RSD) as an indicator of fit.

3 Results and Discussion

3.1 Urban forest structure and distribution

Between LULC types there were distinct differences in the distribution of canopy area, degree of canopy fragmentation, and tree biomass, all of which can be expected to influence the annual rate of long-term C uptake to biomass. Canopy covered 25% of the total study area, of which 85% was within 10 m of an edge, the approximate equivalent of the width of 1–2 mature tree crowns (Pretzsch et al., 2015) (Figure 2). Developed and High-Density Residential areas covered 38% and 39% of the study area, respectively, containing 15% and 46% of total canopy area, of which 97% and 98% was within 10 m of an edge (Table S5). Areas classed Forest occupied only 8% of the study area, but contained 26% of the total urban canopy and 32% of total biomass, of which only 50% was within 10 m of an edge.

The distribution of biomass and canopy coverage implies that while small tracts of Forest-classed land in Boston provide a disproportionate share of services related to canopy and biomass, trees present in the more extensive areas of human-dominated land cover also make a large contribution. Unlike in Forest-classed land, however, trees distributed in these developed and residential areas are likely to function nearly entirely under scattered open-grown condition. Additionally, 50% of biomass in even relatively intact Forest areas still may be under the influence of canopy edge effects. The co-occurrence of both fragments of clustered forest with extensive canopy edges and open-canopy scattered trees suggests that both types of growing contexts need to be accounted for in estimating urban forest ecosystem function.

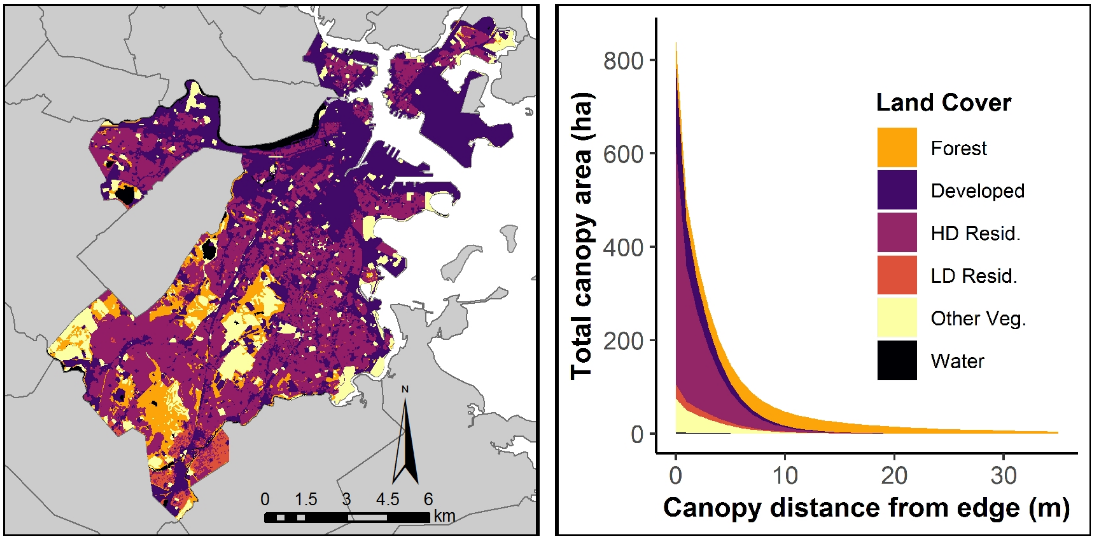

Figure 2: Land-use/land-cover and distribution of canopy area by distance from canopy edge in Boston study area.

3.2 Biomass gain in urban growth contexts

Local stem growth measurements showed growing context had an effect on annual rate of biomass gain per stem, indicating that urban trees may be expected to exhibit different C uptake dynamics depending on setting, and differing from local closed-canopy rural forests. Tree stem growth rate was highest and most variable in Street Trees, with median annual growth rate of 0.73 (-0.49–2.22) cm tree^{-1} yr^{-1} corresponding to median DBH of 25.9 (7.6–71.1) cm. The best-fit mixed model for Street Tree stem growth (RSD = 0.59) showed a significant decline in annual DBH increment with increasing DBH (Figure 3; Table S2). In Urban Forest trees, median DBH increment of edge (<10 m) and interior stems was 0.45 (0.09–1.10) and 0.30 (0.06–0.71) cm tree^{-1} yr^{-1}, corresponding to median DBH of 18.7 (6.3–64.1) cm and 18.8 (7.3–40.7) cm, respectively. The Urban Forest model (RSD = 0.08) predicted faster stem growth than the Rural Forest model, and included a significant predicted increase in growth in stems growing within 10 m of a canopy edge. Growth rates in Street Trees and Urban Forest stems were comparable to the range observed for other trees growing along streets and in green spaces in Bolzano, Italy, (Russo et al., 2014); Leipzig, Germany (Strohbach et al., 2012); and Boston, USA (Briber et al., 2015).

In contrast to the urban-specific growth models, the Rural Forest model (RSD = 0.19) predicted slower stem growth than Urban Forest or Street Trees, with median growth rate of 0.20 (0–0.64) cm tree^{-1} yr^{-1}, corresponding to median DBH 22.6 (13.0–52.1) cm. The range and median of stem DBH in each growth context were similar, except for a lack of trees 5–12 cm DBH range in the Rural Forest due to sampling design. Unlike the Rural- and Urban Forest samples, the Street Tree sample included few conifers and a relatively large fraction of non-local taxa, including members of *Ginkgo, Gleditsia, Pyrus, Tilia* and *Zelkova* (Table S4).

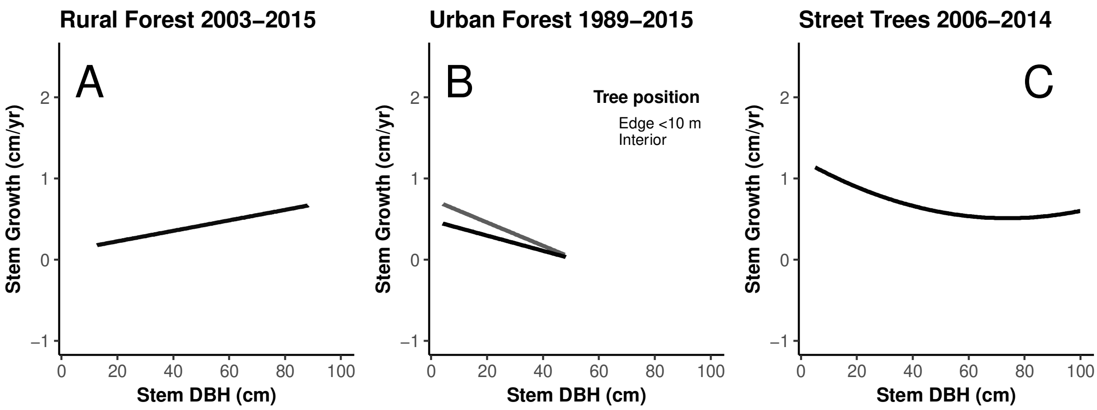

Figure 3: Stem DBH and DBH increment for Rural Forest (A), Urban Forest (B) and Street Tree (C) contexts. Lines show best-fit growth model and shaded area shows 95% confidence interval, and for Urban trees are shaded to show model fit for trees at Edge <10 m (light) and Interior (dark) positions.

Projecting modeled stem growth rates for stems ≥5 cm DBH, median areal-basis growth rate in Urban Forest plots was 0.035 (-0.009–0.062) MgC yr^{-1} per MgC-biomass in edge subplots (<10 m) and 0.024 (-0.010–0.054) MgC yr^{-1} per MgC-biomass in interior subplots (10–30 m) (Table S2). In the final map calculations, pixel-level growth growth predictions under the Urban Forest model were restricted to a range of ±1 SD of the projected maximum and minimum plot-basis growth rates estimated across stem growth models, and estimated uptake values less than 10 kgC yr^{-1} were set to 0 (Supplemental). These growth rates corresponded to plot biomass density of 103.7 (87.8–292.4) and 87.5 (53.8–167.0) MgC ha^{-1} in edge and interior subplots, respectively, based on the total biomass in stems ≥5 cm DBH measured in 2015 in each plot. Both edge and interior subplots showed a significant negative effect of biomass density on areal-basis growth rate, with a significantly lower intercept for interior plots. In Rural Forest plots, areal-basis biomass growth rate was 0.018 (0.004–0.069) MgC yr^{-1} per MgC-biomass with median plot biomass density of 86.4 (33.6–193.0) MgC ha^{-1}. Rural Forest plots showed a significant negative effect in log-biomass growth rate with increasing plot biomass density.

3.3 Effect of biomass density areal basis

This study used areal biomass density (MgC ha^{-1}) to predict local C uptake rate to long-lived biomass. In non-urban forest ecosystems this areal biomass density is in part a product of stand age and successional status, which are also predictive of the rate of net biomass gain in the stand (Ryan et al., 1997). In the scattered canopy and mixed impervious cover of Boston's urban forest, however, the areal basis used in determining biomass density for any given pixel faced potential ambiguity, making the calculated C uptake sensitive to the areal standard chosen. An example of typical discontinuous urban canopy in the study area shows that at moderate levels of both canopy and impervious cover, estimates of biomass density in a given area varied from 22.4 MgC per ha-ground to 89.0 MgC per ha-canopy to 179.3 MgC per ha-pervious (Figure 4). In the same sample area mean Landsat 30 m NDVI was 0.40 (0.22–0.57), comparable to partially vegetated areas, though the area contains appreciable biomass. The comparatively low biomass density on a per-ha-ground basis stood in contrast to the per-ha-pervious density basis, showing unrealistically high biomass density probably resulting from large areas of tree biomass growing over impervious cover.

Because of this areal-basis ambiguity, Rural Forest results using the ground-basis (raw pixel area) for biomass density gave a higher total estimate for biomass C uptake than canopy-basis calculations (Table 1). This result, while closer to the Hybrid Forest model accounting for urban growth rates and growing context, likely does not reflect underlying urban-affected ecosystem dynamics but is rather an artifact of the calculation basis. The lower biomass density calculated on the ground-basis would tend to generate higher predicted rates of relative biomass gain per pixel, with growth parameters more akin to an early stage of forest succession containing more, smaller, faster-growing trees rather than reflecting the true condition of fewer, discontinuous, larger trees.

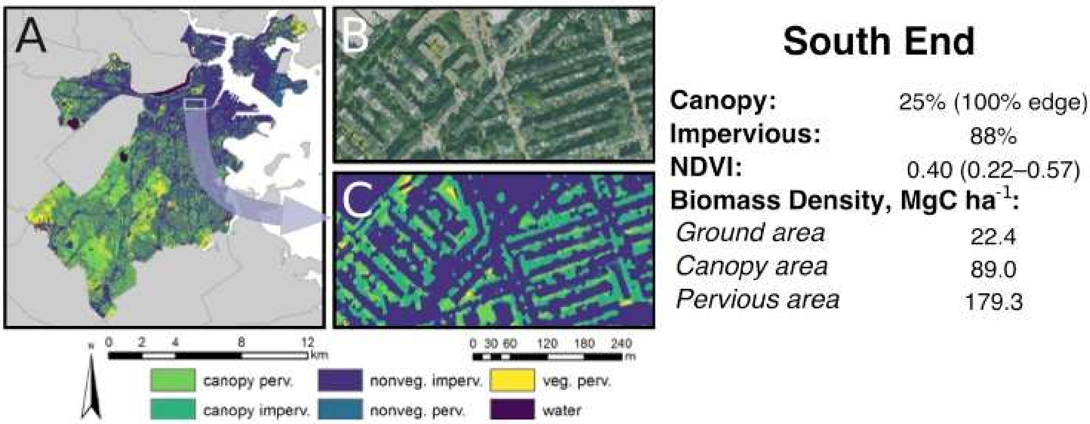

Figure 4: (A) Distribution of vegetation and cover in the study area; (B) Aerial photo of inset area in South End neighborhood (courtesy of USDA National Agriculture Imagery Program); (C) Vegetation and cover type in inset: Canopy over pervious, canopy over impervious, non-vegetated impervious, non-vegetated pervious, vegetated pervious (non-canopy), and open water. Text figures correspond to features of inset area.

3.4 Estimates of annual biomass C uptake

Applying the combined Hybrid Urban model to tree biomass distribution across the city of Boston, we estimated considerably higher annual tree biomass C uptake compared to estimates based on rural growth rates (Rural Forest). The Hybrid Urban model estimated C uptake to long-lived biomass of 10.9 (6.7–16.2) GgC yr^{-1}, with a median uptake rate per pixel of 0.5 (0–3.1) MgC ha^{-1} yr^{-1} across the study area (Table 1). The largest total biomass gains accrued to the Forest, Developed, and HD Residential land use types. By comparison, applying Rural Forest growth factors to per-ha-canopy biomass density showed lower biomass gain in all land use categories, with a median total of 4.8 (3.6–6.4) GgC yr^{-1} and a greater relative fraction of total biomass gain accruing to Forest-classed areas. This reduced estimate of C uptake, particularly in non-Forest cover types, is partly the result of lower per-stem and per-area biomass gain in Rural Forest context than in Urban Forest or Street Trees. In contrast to C uptake on the basis of ground area, aggregating to the total amount of canopy area city-wide shows annual biomass uptake figures were 3.5 (2.1–5.2) MgC per ha-canopy in the Hybrid Urban compared to 1.5 (1.1–2.0) MgC per ha-canopy in the Rural Forest model. The Hybrid Urban results are somewhat lower than tree C uptake per ha-canopy estimated in Los Angeles and Sacramento (McPherson et al., 2013), but may reflect the effects of different species present, growing season length, and climatic conditions. The California study does, however, confirm the relatively high C uptake potential of trees present in mature residential neighborhoods. In contrast, the C uptake estimates from this study are generally higher than the estimate reported for the city of Boston developed under the UFORE method of 2.3 (1.8–2.8) MgC per ha-canopy (Nowak et al., 2013). The Rural Forest model applied to per-ha-ground biomass density produced somewhat higher map-wide total C uptake estimates (Table 1) and higher median estimates of C uptake per pixel (not shown), but this was likely an artifact of the biomass density calculation.

Table 1: Estimated city-wide annual biomass C uptake, and distribution of median per-pixel rate of C uptake (central 95%). Relative areas of LULC types are Forest: 8%; Developed: 38%; HD Resid.: 39%; LD Resid. 2%; Other Veg.: 11%; Water: 2%; Total area: 12,455 ha (See Table S5).

Land use/cover	Biomass C uptake ($GgC\ yr^{-1}$)			Median pixel C uptake ($MgC\ ha^{-1}\ yr^{-1}$)	
	Hybrid Urban	*Rural Forest, canopy basis*	*Rural Forest, ground basis*	*Hybrid Urban*	*Rural Forest, canopy basis*
Forest	2.2 (1.0–5.0)	1.2 (0.9–1.7)	1.4 (1.1–1.9)	2.2 (0.6–3.5)	1.3 (0.3–1.6)
Developed	1.8 (1.0–2.5)	0.7 (0.5–0.9)	1.1 (0.9–1.4)	0.1 (0–2.1)	0 (0–1.0)
HD Resid.	5.3 (2.9–7.8)	2.2 (1.7–3.0)	3.5 (2.8–4.3)	0.9 (0–2.7)	0.4 (0–1.3)
LD Resid.	0.4 (0.2–0.6)	0.2 (0.1–0.2)	0.2 (0.2–0.3)	1.5 (0.2–3.5)	0.7 (0–1.4)
Other Veg.	1.0 (0.6–1.4)	0.4 (0.3–0.5)	0.6 (0.5–0.8)	0.3 (0–3.2)	0.1 (0–1.3)
Water	0.1 (0–0.1)	0 (0–0)	0 (0–0.1)	0 (0–2.5)	0 (0–0.1)
Total	10.9 (6.7–16.2)	4.8 (3.6–6.4)	7.0 (5.6–8.7)	0.5 (0–3.1)	0.2 (0–1.5)

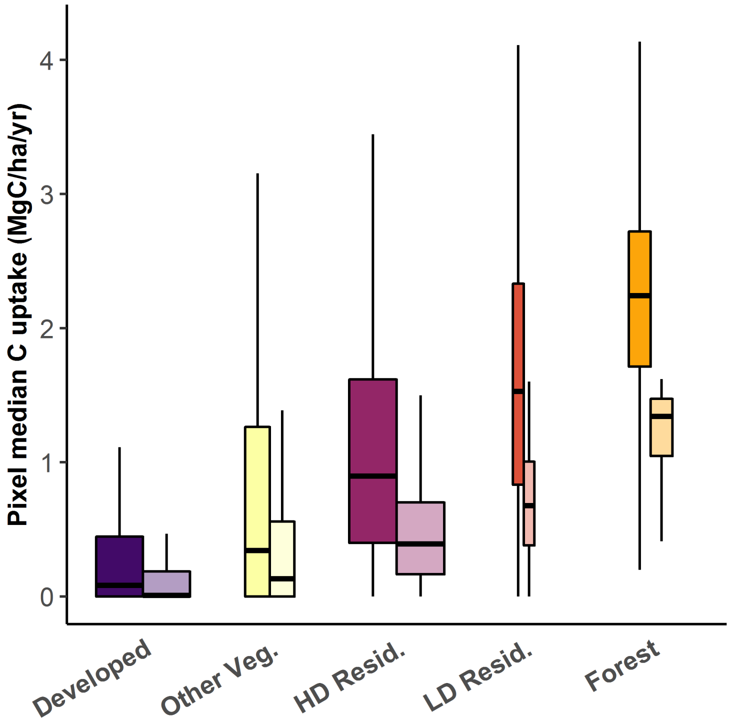

Figure 5: Pixel median biomass C uptake rate (MgC ha^{-1} yr^{-1}) for Hybrid Urban model (dark) and Rural Forest model, canopy basis (light). Box width is proportional to total area of LULC (outliers not shown).

The distribution of pixel median estimates was higher in every LULC category under the Hybrid Urban model (Figure 5). Much of the variation among LULC categories in per-pixel median C uptake was a result of the underlying distributions of pixel biomass. However, persistently higher growth rates modeled for street trees and urban forest fragments in the Hybrid Urban model also contributed to both greater overall spread in per-pixel estimates and higher median biomass C uptake in each LULC category. Much of the HD- and LD Residential pixel population had estimated C uptake at least as large as Forest-classed pixels, even after accounting for higher growth in forest edge biomass. The potential for large biomass C uptake rates in some high-biomass non-forest pixels implies that parts of urban Boston not recognized as forested may be responsible for as at least as much C uptake per ha as local urban forest fragments.

3.5 Policy effects on ecosystem function

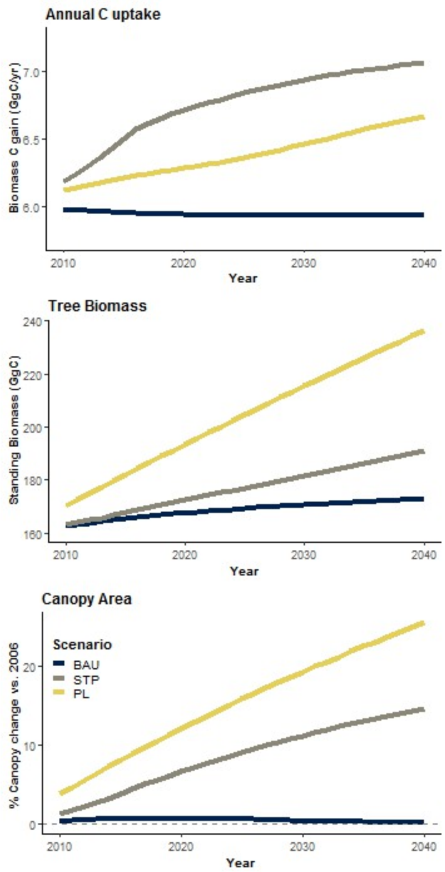

Figure 1: Median projections of annual net C uptake (top), total tree biomass (middle) and change in canopy area from 2006–2040 (bottom) in non-forested Developed, HD Residential, and LD residential pixels. Scenarios tested were Business-as-usual (BAU), Preserve Largest (PL) and Street Tree Planting (STP) from 2006–2040.

Policies for preserving larger trees (PL) and for expanding street trees numbers in plantable roadside areas (STP) resulted in differential gains in biomass C uptake, total biomass, and canopy cover by 2040 relative to Business-as-usual BAU, had these different policies been implemented starting in 2006 (Figure 6). Median projected annual C uptake by 2040 was highest under STP at 7.1 (3.6–11.8) GgC yr^{-1} and rose relatively rapidly over the initial 10 years of simulated tree planting, but also continued to rise under PL up to 6.7 (2.8–14.1) GgC yr^{-1}, compared to BAU which declined slowly to 5.9 (2.9–10.4) GgC yr^{-1}. In contrast, projected biomass and change in canopy cover change relative to 2006 both rose most mostly rapidly under PL, reaching a median of 236 (148–343) GgC and +25% (-6–54%), compared to more modest increases under STP to 191 (129–257) GgC and +15% (-8–37%) by 2040, respectively. Under BAU by comparison, 2040 median projected biomass remained roughly stable at 173 (117–235) GgC, and showed a median stable canopy cover change of 0% (-20–20%). The variability in the projected results reflects the stochastic occurrence of individual tree mortalities in each pixel simulation, variability in the simulated collections of tree stems present at the pixel level, and estimation error in the underlying Street Tree growth model.

Differential changes in urban forest demographics likely caused these divergent policy effects on the ecosystem functional metrics. Under the PL policy, simulator results from 2006–2040 showed the cumulative sum of mortality events was lower (487×10^3 [$473–508 \times 10^3$]) and final 2040 city-wide number of living trees was somewhat higher (552×10^3 [$550–554 \times 10^3$]) compared to BAU mortalities (583×10^3 [$578–592 \times 10^3$]), and final number (546×10^3 [$545–548 \times 10^3$]). These results likely reflect the reduction in tree mortality and higher equilibrium tree population expected under PL as the simulated tree populations matured into larger DBH classes >40 cm with lower mortality as a result of the policy. Since the policy simulations all assumed complete replacement of dead trees with new small trees, total mortalities could be comparable to the total number of living trees as the result of this ongoing turnover in the tree population (Supplemental). The greater percentage of high-biomass/high-canopy area trees under PL is therefore likely the cause of the greater projected gains in 2040 biomass and relative canopy change. In contrast, under the STP policy median tree number expanded to 666×10^3 ($665–668 \times 10^3$) with 126×10^3 ($125–126 \times 10^3$) new live stems installed in suitable areas of road buffer. Though these greater stem numbers lifted total mortalities under STP (700×10^3 [$694–708 \times 10^3$]), the addition of new growing biomass also caused median annual biomass C uptake by 2040 to exceed median uptake under PL. However, the addition of smaller trees under STP was not sufficient to surpass the median projected gains in live biomass and canopy cover predicted with the shift to a higher fraction of larger trees under PL. Overall stability, or potential loss, in canopy cover and biomass C uptake in the absence of these policy interventions under BAU, even with prompt and complete replanting of mortalities, could be a product of mortality losses of vulnerable larger trees causing a demographic shift towards smaller more recently planted stems (Smith et al., 2019).

Our assumption of no canopy overlap or other interferences on canopy area growth may not hold in in areas with high tree or building density, and canopy area may be less precisely estimated at the extreme upper end of the range of individual stem DBH. The prediction of a continued strong upward trend in growth in canopy area under PL may as a consequence somewhat overestimate the potential for continuous expansion in canopy cover as the result of continuous canopy growth in large-diameter trees across the city. Similarly with annual C uptake and total biomass, there is likely an upper limit to the size and growth rate of large urban trees that would imply that the continued positive trends in these metrics under PL may not be maintained over a sufficiently long time scale. Conversely, the positive functional trends under STP represent the outcomes of an aggressive program of tree expansion, simultaneous with the complete replacement of ongoing tree mortalities. The practical efficacy of potential of tree planting programs in Boston and elsewhere remain uncertain and the topic of study (Danford et al., 2014; O'Neil-Dunne, 2017). The functional trends under PL and STP may therefore represent the upper envelope for the magnitude of impacts under policies similar to these. While marginal adjustments to the assumptions of the projections might alter the relative performances of PL and STP, the simulation results do suggest, however, that either policy intervention would lead to greater values in these ecosystem functional metrics relative to BAU over time.

4 Conclusions

The results of this study highlight the impact that altered ecosystem functions in urbanized landscapes might have on some of the services performed by urban vegetation. Scaling up local measurements of stem growth rate with reference to canopy configuration, we find that estimated biomass C uptake in the city of Boston could be substantially greater than estimates treating tree growth as similar to rural forest analogues. Accounting for this urban growth context in C uptake requires putting traditional ecosystem metrics like biomass density and canopy edge configuration into its realistic spatial context, given the heterogeneity and fragmented nature of the urban forest. These differences in function have implications for municipal policy toward managing and optimizing their services. Projecting different urban tree policies through 2040, we find that preserving larger trees may tend to maximize the functions of canopy cover and biomass C storage, while new tree planting may help maximize biomass C uptake capacity. The present uncertainties in quantifying urban ecosystem function or in predicting responses to policy call for more complete and frequent monitoring of basic indicators of urban forest function, such as regular urban street tree census and aerial observations of canopy extent (O'Neil-Dunne, 2017).

Though remaining forest fragments in Boston contained a relatively large fraction of total biomass and canopy coverage given their small areas, the bulk of urban tree biomass was present in densely developed residential areas. As such, this type of land cover/use is likely to host to a significant portion of some of the ecosystem services provided by the city's urban trees. The large extent of this open-canopy "urban savannah" dominated by trees in planters, private yards, and along streets implies that municipal-scale policy focused only on identifiable green spaces like parks and preserves will fail to address services provision by a large portion of urban tree biomass and canopy extent—particularly services like temperature moderation whose value is limited by proximity to people (Ziter et al., 2019). The results of our policy projections offer hope that optimizing local ecosystem services could be achieved by addressing uniquely urban factors of tree growth and demographics, such as heightened mortality, uneven stand age structure, and simple lack of trees in available growing space. In addition, the finding of potentially declining functional indicators under a "Business-as-Usual" policy prescription also underlines the reality that urban forests are dynamic systems, facing both the combined effects of changing global climate and intensifying local urban climate effects. Even maintaining present services may require active social intervention over the next few decades.

Our study suggests that though biogenic C uptake in some parts of the city may be comparable to rates in intact forest, these localized C sinks do not in sum amount to a large overall offset to Boston's CO_2 emissions, with annual tree CO_2-equivalent uptake at a maximum of 0.8% of the total 6.9 million tonnes of CO_2-eq emissions for the city in 2016 (City of Boston, 2016). On the other hand, cities that have made emissions reductions pledges also face the need to monitor progress towards these goals. Unfortunately, atmospheric methods under development for monitoring regional urban CO_2 emissions still face considerable ambiguity during the growing season due to interference from poorly quantified and spatially resolved urban biogenic C fluxes (Sargent et al., 2018). Resolving and contextualizing these potent but spatiotemporally localized sinks (Hardiman et al., 2017; Miller et al., 2018), could directly benefit these emissions monitoring efforts. A more complete accounting of urban biogenic C flux would estimate not only short- and long-term C uptake by tree tissues but also non-tree vegetation C uptake, while incorporating auto- and heterotrophic respiration C release processes that also vary in time and space and in response to specific urban conditions (Decina et al., 2016; Wang et al., 2017). Future research should quantify these important urban biogenic C flux components and their relationships with urban forest ecosystem services more broadly to provide an improved spatiotemporal picture of urban biogeochemical C cycling—one that will advance our capacity to monitor anthropogenic C emissions and better assess progress in mounting municipal-scale climate change responses.

Acknowledgements: This work was supported by the National Oceanic and Atmospheric Agency grant NA14OAR4310179 and the National Aeronautics and Space Administration grant NNX16AP23G. The authors acknowledge Dr. Steve M. Raciti for the public availability of the biomass and canopy data as well as consultation he provided on their construction. The authors also acknowledge Dr. Chloe Anderson, Dr. Kira Sullivan-Wiley, and Ana Reboredo Segovia for comments on early drafts of this work. We also wish to thank the two anonymous reviewers of this manuscript for their detailed and helpful comments prior to publications.

CRediT author statement

Andrew Trlica: Conceptualization, Formal Analysis, Methodology, Software, Writing – Original Draft, Writing – Review and editing. **Lucy R. Hutyra:** Funding Acquisition, Supervision, Writing – Review and editing. **Luca L. Morreale:** Data curation, Writing – Review and editing. **Ian A. Smith:** Data curation, Methodology, Writing – Review and editing; Andrew B. Reinmann: Data curation, Writing – Review and editing

References

Alberti, M., 2015. Eco-evolutionary dynamics in an urbanizing planet. Trends in Ecology and Evolution 30, 114–126. https://doi.org/10.1016/j.tree.2014.11.007

Bellucco, V., Marras, S., Grimmond, C.S.B., Järvi, L., Sirca, C., Spano, D., 2017. Modelling the biogenic CO2 exchange in urban and non-urban ecosystems through the assessment of light-response curve parameters. Agricultural and Forest Meteorology 236, 113–122. https://doi.org/10.1016/j.agrformet.2016.12.011

Brack, C.L., 2002. Pollution mitigation and carbon sequestration by an urban forest. Environmental Pollution 116. https://doi.org/10.1016/S0269-7491(01)00251-2

Briber, B.M., Hutyra, L.R., Reinmann, A.B., Raciti, S.M., Dearborn, V.K., Holden, C.E., Dunn, A.L., 2015. Tree productivity enhanced with conversion from forest to urban land covers. PLoS ONE 10, 1–19. https://doi.org/10.1371/journal.pone.0136237

Broto, V.C., Bulkeley, H., 2013. A survey of urban climate change experiments in 100 cities. Global Environmental Change 23, 92–102. https://doi.org/10.1016/j.gloenvcha.2012.07.005

Castán Broto, V., 2017. Urban Governance and the Politics of Climate change. World Development 93, 1–15. https://doi.org/10.1016/j.worlddev.2016.12.031

Crawford, B., Grimmond, C.S.B., Christen, A., 2011. Five years of carbon dioxide fluxes measurements in a highly vegetated suburban area. Atmospheric Environment 45, 896–905. https://doi.org/10.1016/j.atmosenv.2010.11.017

Danford, R.S., Strohbach, M.W., Ryan, R., Nicolson, C., Warren, P.S., 2014. What does it take to achieve equitable urban tree canopy distribution? A Boston case study. Cities and the Environment 7, Article 2.

Davies, Z.G., Edmondson, J.L., Heinemeyer, A., Leake, J.R., Gaston, K.J., 2011. Mapping an urban ecosystem service: Quantifying above-ground carbon storage at a city-wide scale. Journal of Applied Ecology 48, 1125–1134. https://doi.org/10.1111/j.1365-2664.2011.02021.x

Decina, S.M., Hutyra, L.R., Gately, C.K., Getson, J.M., Reinmann, A.B., Short Gianotti, A.G., Templer, P.H., 2016. Soil respiration contributes substantially to urban carbon fluxes in the greater Boston area. Environmental Pollution 212, 433–439. https://doi.org/10.1016/j.envpol.2016.01.012

Dobbs, C., Nitschke, C., Kendal, D., 2017. Assessing the drivers shaping global patterns of urban vegetation landscape structure. Science of the Total Environment 592, 171–177. https://doi.org/10.1016/j.scitotenv.2017.03.058

Escobedo, F.J., Kroeger, T., Wagner, J.E., 2011. Urban forests and pollution mitigation: Analyzing ecosystem services and disservices. Environmental Pollution 159, 2078–2087. https://doi.org/10.1016/j.envpol.2011.01.010

Escobedo, F.J., Nowak, D.J., 2009. Spatial heterogeneity and air pollution removal by an urban forest. Landscape and Urban Planning 90, 102–110. https://doi.org/10.1016/j.landurbplan.2008.10.021

Fahey, T.J., Siccama, T.G., Driscoll, C.T., Likens, G.E., Campbell, J., Johnson, C.E., Battles, J.J., Aber, J.D., Cole, J.J., Fisk, M.C., Groffman, P.M., Hamburg, S.P., Holmes, R.T., Schwarz, P.A., Yanai, R.D., 2005. The biogeochemistry of carbon at Hubbard Brook. Biogeochemistry 75, 109–176. https://doi.org/10.1007/s10533-004-6321-y

Gómez-Baggethun, E., Barton, D.N., 2013. Classifying and valuing ecosystem services for urban planning. Ecological Economics 86, 235–245. https://doi.org/10.1016/j.ecolecon.2012.08.019

Gregg, J.W., Jones, C.G., Dawson, T.E., 2003. Urbanization effects on tree growth in the vicinity of New York City. Earth 424, 183–187. https://doi.org/10.1038/nature01776.1.

Groffman, P.M., Cadenasso, M.L., Cavender-Bares, J., Childers, D.L., Grimm, N.B., Grove, J.M., Hobbie, S.E., Hutyra, L.R., Darrel Jenerette, G., McPhearson, T., Pataki, D.E., Pickett, S.T.A., Pouyat, R. V., Rosi-Marshall, E., Ruddell, B.L., 2017. Moving Towards a New Urban Systems Science. Ecosystems 20, 38–43. https://doi.org/10.1007/s10021-016-0053-4

Hardiman, B.S., Wang, J.A., Hutyra, L.R., Gately, C.K., Getson, J.M., Friedl, M.A., 2017. Accounting for urban biogenic fluxes in regional carbon budgets. Science of the Total Environment 592, 366–372. https://doi.org/10.1016/j.scitotenv.2017.03.028

Hutyra, L.R., Duren, R., Gurney, K.R., Grimm, N., Kort, E.A., Larson, E., Shrestha, G., 2014. Urbanization and the carbon cycle : Current capabilities and research outlook from the natural sciences perspective Earth ’ s Future. Earth’s Future 2, 473–495. https://doi.org/10.1002/2014EF000255

Hutyra, L.R., Yoon, B., Hepinstall-Cymerman, J., Alberti, M., 2011. Carbon consequences of land cover change and expansion of urban lands: A case study in the Seattle metropolitan region. Landscape and Urban Planning 103, 83–93. https://doi.org/10.1016/j.landurbplan.2011.06.004

Imhoff, M.L., Bounoua, L., DeFries, R., Lawrence, W.T., Stutzer, D., Tucker, C.J., Ricketts, T., 2004. The consequences of urban land transformation on net primary productivity in the United States. Remote Sensing of Environment 89, 434–443. https://doi.org/10.1016/j.rse.2003.10.015

Kremer, P., Hamstead, Z.A., McPhearson, T., 2016. The value of urban ecosystem services in New York City: A spatially explicit multicriteria analysis of landscape scale valuation scenarios. Environmental Science and Policy 62, 57–68. https://doi.org/10.1016/j.envsci.2016.04.012

Larondelle, N., Haase, D., 2013. Urban ecosystem services assessment along a rural-urban gradient: A cross-analysis of European cities. Ecological Indicators 29, 179–190. https://doi.org/10.1016/j.ecolind.2012.12.022

Lovell, S.T., Taylor, J.R., 2013. Supplying urban ecosystem services through multifunctional green infrastructure in the United States. Landscape Ecology 28, 1447–1463. https://doi.org/10.1007/s10980-013-9912-y

Magill, A.H., Aber, J.D., Currie, W.S., Nadelhoffer, K.J., Martin, M.E., McDowell, W.H., Melillo, J.M., Steudler, P., 2004. Ecosystem response to 15 years of chronic nitrogen additions at the Harvard Forest LTER, Massachusetts, USA. Forest Ecology and Management 196, 7–28. https://doi.org/10.1016/j.foreco.2004.03.033

McDonald, R.I., Kroeger, T., Zhang, P., Hamel, P., 2019. The Value of US Urban Tree Cover for Reducing Heat-Related Health Impacts and Electricity Consumption. Ecosystems. https://doi.org/10.1007/s10021-019-00395-5

McPherson, E.G., Qingfu, X., Elena, A., 2013. A new approach to quantify and map carbon stored , sequestered and emissions avoided by urban forests. Landscape and Urban Planning 120, 70–84. https://doi.org/10.1016/j.landurbplan.2013.08.005

McPherson, E.G., Van Doorn, N.S., Peper, P.J., 2016. Urban Tree Database and Allometric Equations. United States Department of Agriculture. https://doi.org/10.2737/RDS-2016-0005

Melaas, E.K., Wang, J.A., Miller, D.L., Friedl, M.A., 2016. Interactions between urban vegetation and surface urban heat islands: a case study in the Boston metropolitan region. Environmental Research Letters 11, 054020. https://doi.org/10.1088/1748-9326/11/5/054020

Miller, D.L., Roberts, D.A., Clarke, K.C., Lin, Y., Menzer, O., Peters, E.B., McFadden, J.P., 2018. Gross primary productivity of a large metropolitan region in midsummer using high spatial resolution satellite imagery. Urban Ecosystems 21, 831–850. https://doi.org/10.1007/s11252-018-0769-3

Niemelä, J., 2014. Ecology of urban green spaces: The way forward in answering major research questions. Landscape and Urban Planning 125, 298–303. https://doi.org/10.1016/j.landurbplan.2013.07.014

Nowak, D.J., Crane, D.E., Stevens, J.C., Hoehn, R.E., Walton, J.T., Bond, J., 2008. A ground-based method of assessing urban forest structure and ecosystem services. Arboriculture and Urban Forestry 34, 347–358. https://doi.org/10.1039/b712015j

Nowak, D.J., Greenfield, E.J., 2012. Tree and impervious cover in the United States. Landscape and Urban Planning 107, 21–30. https://doi.org/10.1016/j.landurbplan.2012.04.005

Nowak, D.J., Greenfield, E.J., Hoehn, R.E., Lapoint, E., 2013. Carbon storage and sequestration by trees in urban and community areas of the United States. Environmental Pollution 178, 229–236. https://doi.org/10.1016/j.envpol.2013.03.019

O'Neil-Dunne, J., 2017. An Assessment of Boston's Tree Canopy, Urban Tree Canopy Assessment.

Ossola, A., Hopton, M.E., 2018. Measuring urban tree loss dynamics across residential landscapes. Science of the Total Environment 612, 940–949. https://doi.org/10.1016/j.scitotenv.2017.08.103

Ouimette, A.P., Ollinger, S. V., Richardson, A.D., Hollinger, D.Y., Keenan, T.F., Lepine, L.C., Vadeboncoeur, M.A., 2018. Carbon fluxes and interannual drivers in a temperate forest ecosystem assessed through comparison of top-down and bottom-up approaches. Agricultural and Forest Meteorology. https://doi.org/10.1016/j.agrformet.2018.03.017

Pataki, D.E., 2013. Urban greening needs better data. Nature 502, 624.

Pataki, D.E., Carreiro, M.M., Cherrier, J., Grulke, N.E., Jennings, V., Pincetl, S., Pouyat, R. V., Whitlow, T.H., Zipperer, W.C., 2011. Coupling biogeochemical cycles in urban environments: Ecosystem services, green solutions, and misconceptions. Frontiers in Ecology and the Environment 9, 27–36. https://doi.org/10.1890/090220

Pataki, D.E., Emmi, P.C., Forster, C.B., Mills, J.I., Pardyjak, E.R., Peterson, T.R., Thompson, J.D., Dudley-Murphy, E., 2009. An integrated approach to improving fossil fuel emissions scenarios with urban ecosystem studies. Ecological Complexity 6, 1–14. https://doi.org/10.1016/j.ecocom.2008.09.003

Pincetl, S., Gillespie, T., Pataki, D.E., Saatchi, S., Saphores, J.D., 2013. Urban tree planting programs, function or fashion? Los Angeles and urban tree planting campaigns. GeoJournal 78, 475–493. https://doi.org/10.1007/s10708-012-9446-x

Pretzsch, H., Biber, P., Uhl, E., Dahlhausen, J., Rötzer, T., Caldentey, J., Koike, T., van Con, T., Chavanne, A., Seifert, T., Toit, B. du, Farnden, C., Pauleit, S., 2015. Crown size and growing space requirement of common tree species in urban centres, parks, and forests. Urban Forestry and Urban Greening 14, 466–479. https://doi.org/10.1016/j.ufug.2015.04.006

Pretzsch, H., Biber, P., Uhl, E., Dahlhausen, J., Schütze, G., Perkins, D., Rötzer, T., Caldentey, J., Koike, T., Con, T. Van, Chavanne, A., Toit, B. Du, Foster, K., Lefer, B., 2017. Climate change accelerates growth of urban trees in metropolises worldwide /631/158/858 /704/158/2165 article. Scientific Reports 7, 1–10. https://doi.org/10.1038/s41598-017-14831-w

Raciti, S.M., Hutyra, L.R., Newell, J.D., 2014. Mapping carbon storage in urban trees with multi-source remote sensing data: Relationships between biomass, land use, and demographics in Boston neighborhoods. Science of The Total Environment 500–501, 72–83. https://doi.org/10.1016/j.scitotenv.2014.08.070

Raciti, S.M., Hutyra, L.R., Rao, P., Finzi, A.C., 2012. Inconsistent definitions of "urban" result in different conclusions about the size of urban carbon and nitrogen stocks. Ecological Applications 22, 1015–1035. https://doi.org/10.1890/11-1250.1

Rao, P., Hutyra, L.R., Raciti, S.M., Finzi, A.C., 2013. Field and remotely sensed measures of soil and vegetation carbon and nitrogen across an urbanization gradient in the Boston metropolitan area. Urban Ecosystems 16, 593–616. https://doi.org/10.1007/s11252-013-0291-6

Reinmann, A.B., Hutyra, L.R., 2017. Edge effects enhance carbon uptake and its vulnerability to climate change in temperate broadleaf forests. Proceedings of the National Academy of Sciences 114, 107–112. https://doi.org/10.1073/pnas.1612369114

Roman, L.A., Battles, J.J., McBride, J.R., 2014. The balance of planting and mortality in a street tree population. Urban Ecosystems 17, 387–404. https://doi.org/10.1007/s11252-013-0320-5

Roman, L.A., Pearsall, H., Eisenman, T.S., Conway, T.M., Fahey, R.T., Landry, S., Vogt, J., Doorn, N.S. Van, Grove, J.M., Locke, D.H., Bardekjian, A.C., Battles, J.J., Cadenasso, M.L., Konijnendijk, C.C., Bosch, V. Den, Avolio, M., Berland, A., Jenerette, G.D., Mincey, S.K., Pataki, D.E., Staudhammer, C., van Doorn, N.S., Grove, J.M., Locke, D.H., Bardekjian, A.C., Battles, J.J., Cadenasso, M.L., van den Bosch, C.C.K., Avolio, M., Berland, A., Jenerette, G.D., Mincey, S.K., Pataki, D.E., Staudhammer, C., 2018. Human and biophysical legacies shape contemporary urban forests: A literature synthesis. Urban Forestry and Urban Greening 31, 157–168. https://doi.org/10.1016/j.ufug.2018.03.004

Roy, S., Byrne, J., Pickering, C., 2012. A systematic quantitative review of urban tree benefits, costs, and assessment methods across cities in different climatic zones. Urban Forestry and Urban Greening 11, 351–363. https://doi.org/10.1016/j.ufug.2012.06.006

Russo, A., Escobedo, F.J., Timilsina, N., Schmitt, A.O., Varela, S., Zerbe, S., 2014. Assessing urban tree carbon storage and sequestration in Bolzano, Italy. International Journal of Biodiversity Science, Ecosystem Services and Management 10, 54–70. https://doi.org/10.1080/21513732.2013.873822

Ryan, M.G., Binkley, D., Fownes, J.H., 1997. Age-Related Decline in Forest Productivity: Pattern and Process. Advances in Ecological Research 27, 213–262. https://doi.org/10.1016/S0065-2504(08)60009-4

Sargent, M., Barrera, Y., Nehrkorn, T., Hutyra, L.R., Gately, C.K., Jones, T., McKain, K., Sweeney, C., Hegarty, J., Hardiman, B., Wang, J.A., Wofsy, S.C., 2018. Anthropogenic and biogenic CO 2 fluxes in the Boston urban region . Proceedings of the National Academy of Sciences 115, 7491–7496. https://doi.org/10.1073/pnas.1803715115

Searle, S.Y., Turnbull, M.H., Boelman, N.T., Schuster, W.S.F.F., Yakir, D., Griffin, K.L., 2012. Urban environment of New York City promotes growth in northern red oak seedlings. Tree Physiology

32, 389–400. https://doi.org/10.1093/treephys/tps027

Seto, K.C., Guneralp, B., Hutyra, L.R., 2012. Global forecasts of urban expansion to 2030 and direct impacts on biodiversity and carbon pools. Proceedings of the National Academy of Sciences 109, 16083–16088. https://doi.org/10.1073/pnas.1211658109

Smith, I.A., Dearborn, V.K., Hutyra, L.R., 2019. Live fast, die young: Accelerated growth, mortality, and turnover in street trees. Plos One 14, e0215846. https://doi.org/10.1371/journal.pone.0215846

Strohbach, M.W., Arnold, E., Haase, D., 2012. The carbon footprint of urban green space-A life cycle approach. Landscape and Urban Planning 104, 220–229. https://doi.org/10.1016/j.landurbplan.2011.10.013

van Doorn, N.S., McPherson, E.G., 2018. Demographic trends in Claremont California's street tree population. Urban Forestry and Urban Greening 29, 200–211. https://doi.org/10.1016/j.ufug.2017.11.018

Wang, J.A., Hutyra, L.R., Li, D., Friedl, M.A., 2017. Gradients of atmospheric temperature and humidity controlled by local urban land-use intensity in Boston. Journal of Applied Meteorology and Climatology 56, 817–831. https://doi.org/10.1175/JAMC-D-16-0325.1

Zhou, W., Fisher, B., Pickett, S.T., 2019. Cities are hungry for actionable ecological knowledge. Frontiers in Ecology and the Environment 17, 135–135. https://doi.org/10.1002/fee.2021

Ziter, C.D., Pedersen, E.J., Kucharik, C.J., Turner, M.G., 2019. Scale-dependent interactions between tree canopy cover and impervious surfaces reduce daytime urban heat during summer. Proceedings of the National Academy of Sciences 116, 7575–7580. https://doi.org/10.1073/pnas.1817561116

Zurr, A., Ieno, E.N., Walker, N., Savliev, A.A., Smith, G.M. 2009. Mixed effects models and extensions in ecology with R. Springer Science+Business Media, LLC. DOI 10.1007/978-0-387-87458-6_19